7. J. W. Rutter and B. Chalmers, Can. J. Phys., **31**, No. 1, 15-39 (1953).
8. G. P. Ivantsov, Dokl. Akad. Nauk SSSR, **81**, No. 2, 179-182 (1951).
9. A. I. Plotnikov, V. A. Loginov, and S. I. Rembeza, Zh. Tekh. Fiz., **60**, No. 12, 131-133 (1990).
10. G. A. Mesyats, Pis'ma Zh. Tekh. Fiz., **9**, No. 14, 891-893 (1983).
11. S. M. Lupekhin, G. N. Fursei, M. A. Polyakov, et al., Pis'ma Zh. Tekh. Fiz., **9**, No. 17, 1978-1080 (1983).
12. V. V. Vladimirov, P. M. Golovinskii, and G. A. Mesyats, Zh. Tekh. Fiz., **57**, No. 8, 1588-1597 (1987).
13. E. A. Litvinov, G. A. Mesyats, and D. I. Proskurovskii, Usp. Fiz. Nauk, **139**, No. 2, 265-302 (1983).
14. L. Tonks, Phys. Rev., **48**, No. 6, 562-568 (1935); Ya. I. Frenkel, Phys. Zs. Sowietunion, **8**, 675-679 (1935).
15. V. V. Valdimirov and P. M. Golovitskii, Zh. Tekh. Fiz., **55**, No. 2, 440-442 (1985).
16. N. I. Dolbin and A. I. Morozov, Zh. Tekh. Fiz., **55**, No. 9, 1849-1854 (1985).
17. G. I. Taylor, Proc. R. Soc. (London), **280A**, No. 1382, 383-397 (1964).
18. Lord Rayleigh, Philos. Mag., **34**, No. 207-145-154 (1892).
19. M. Faraday, Philos. Trans. R. Soc. Ser. Math. Phys. Sci., **121**, 299-340 (1831).
20. V. V. Vladimirov, V. N. Gorshkov, V. N. Zamkov, et al., Zh. Tekh. Fiz., **61**, No. 1, 197-200 (1991).

# THERMAL TURBULENCE IN AN ELECTRIC ARC

**T. V. Laktyushina, G. P. Lizunkov, and O. I. Yas'ko**

UDC 533.951.7

*By analyzing the correlations of current–voltage characteristics we show the predominance of turbulent heat exchange by convection and conduction in a longitudinally blown helium arc. The presence of "thermal" turbulence in the near-axial zone of this arc has been verified experimentally by investigating the radiation intensity.*

In the process of developing and utilizing electric arc plasma devices, the nature of flow of the plasma flux, on which the arc interaction with the heated medium in the discharge chamber of the plasmotron has a decisive effect, is very important. The presence of an intense source of heat release, such as an electric arc, complicates substantially the nature of flow of the operating medium in a discharge channel in comparison with a cold flux without an arc discharge. To determine the flow regime in this case it is insufficient to simply compare the Reynolds number with its critical value.

Firstly, the plasma flux density in an arc column $\rho_{pl}v_{pl}$ is lower than in a heated cold flux $\rho_{cld}v_{cld}$. This leads to some reduction in the decisive size. Secondly, the heating of the operating medium increases strongly the flux viscosity. Therefore, the actual meaning of the Re number is much more restricted than when it is determined from "cold" parameters. Consequently, the calculation of the Reynolds criterion from the mean-mass temperature has become widely used. This method, however, is far from perfect, since the mean-mass temperature is not the primary given parameter, while the temperature itself depends on the operating regime of the device – the current intensity, the gas discharge, the pressure, and the geometry of the discharge channel. Consequently, the determination of the Re number value from the mean-mass parameters is the essential parameter, i.e., it is not an independent generalized argument.

There also exists an additional complication, besides the difficulties mentioned. In an electric arc there exist intrinsic instability sources of thermal and electric nature. More precisely, these play a more substantial role than the interaction forces on which the Reynolds number depends. An attempt of generalizing its current–voltage characteristics (CVC) [1, 2] is an indication of the decisive effect of energy exchange processes on the properties of arc discharge. Obviously, the effect of energy

Academic Scientific Complex, A. V. Lykov Institute of Heat and Mass Transfer, Belarus Academy of Sciences, Minsk.
Translated from Inzhenerno-Fizicheskii Zhurnal, Vol. 62, No. 5, pp. 691-700, May, 1992. Original article submitted November 12, 1991.

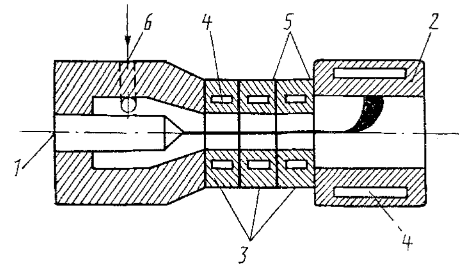


Fig. 1. Sketch of experimental plasmotron: 1) cathode bar, 2) cylindrical anode, 3) discharge channel of water-cooled washers, 4) circulation channel in washers for water cooling, 5) isolating spacers, 6) gas-conducting channel.

exchange processes on the flow regime must be accounted for not by the Reynolds number, but by some other criterion of "thermal turbulence." Such a number was suggested in [3, 4] on the basis of using a method of dimensionality analysis.

The purpose of the present study is to explain the physical essence of the energy exchange process in thermal turbulence. Although thermal destabilization of electric discharges is theoretically understood [5, 6], experimental studies of this effect are so far scarce. In this case one usually treats only one aspect of the problem, such as temperature fluctuations [7]. An attempt is made in the present study to compare data of spectral and interferometric studies of temperature instabilities in electric arc discharges with analysis of energy exchange processes by a correlation method of CVC of an arc.

**1. Experimental Studies. Experimental Devices.** To investigate parameter instabilities, an electric arc of constant current was ignited in a cylindrical channel, containing water-cooled copper washers of thickness 5 mm, isolated from each other (Fig. 1). The channel diameters were 8 and 10 mm, and the channel lengths were 50 and 100 mm. The isolation thickness between washers (mica, paranite, plastic) was 0.3-2.0 mm. A copper anode bar was used. The channel was blown with different gases: argon (G = 0.3-3.5 g/sec), helium (0.1-0.5), nitrogen (0.5-4.0), and air (1.0-4.0). The current varied from 60 to 250 A.

The recording of radiation with temporal $10^{-6}$ sec and spatial $10^{-5}$ m resolutions was implemented by automated complexes, in particular a television system in which a transmission chamber with a vidicon was placed at the monochromator output [8]. The signal was suppressed by the chamber at the control on the television screen and on an oscillograph, with which the image was photorecorded by a fast cine-camera, synchronized with a shutter. At the same time, on the oscillograph screen one can place from 1 to 6 independently selected oscillograms, which made it possible to record the spatial distribution of the radiation intensity in several spectral regions.

The interferometric measurements were carried out by a specially designed device [9], providing protection from vibration and removing distortions due to observation windows at the discharge chamber. For these observation windows of the chamber we provided interferometric tapered semitransparent mirrors, forming reference and object beams. Removal of vibrations was guaranteed by attaching the mirrors to the chamber walls by rubber sealing rings. The recording of interference fringes was implemented by an SFR fast cine-camera with a speed up to $2.5 \cdot 10^5$ frames/sec.

To extract the current–voltage characteristics of the arc discharge we used plasmotrons guaranteeing parameter variation within wider limits. The diameter of the discharge chamber varied from 10 to 40 mm, the current intensity – from 40 to 900 A, argon discharge – from 1 to 12 g/sec, helium – from 0.25 to 4 g/sec, nitrogen – from 2 to 6 g/sec, and air – from 0.35 to 15.25 g/sec. Besides, the CVC was also extracted for an arc blown by hydrogen with a discharge from 1 to 3 g/sec. In this case it was not necessary to use a sectional diaphragm of separate isolated washers, and it was prepared in the form of a solid water-cooled cylinder.

**Spatial Oscillations of an Arc Column.** The arc photorecordings show that for small gas discharges it is particularly noticeable in argon for G = 0.3-0.5 g/sec at the channel origin ($l/d$ = 2.5-3.0), and stable heating is observed without substantial column deviation from the axis. The instability gradually increases with increasing gas discharge and distance from the cathode for a given current value: transverse column displacements occur, as well as fluctuations in the radiant flux and in the arc diameter. The diameter increases with increasing current at constant discharge, but the random oscillations decrease.

Regular arc oscillations, whose frequencies depend on the geometric shape of the channel, the nature of the gas, its discharge, and the current intensity, are also observed. Intense random displacements of the arc column are observed in nitrogen and air at relatively low currents (I = 70-150 A) and high discharges (G = 1-2 g/sec). Periodicities are generated on the background of random oscillations for currents increasing up to 220 A and low discharges (G = 1 g/sec). This process is manifested even more strongly in helium (G = 0.1-0.3 g/sec, I = 140-160 A), where the depth of radiation modulation is larger by 3-5 times than in nitrogen or argon. Regular oscillations with frequency 4 kHz appear in helium at G = 0.1 g/sec in an 8 mm channel with a slot (cylindrical deepening d = 20-30 mm, h = 1-2 mm). Oscillations of frequency 12 kHz are also generated with gas discharge increasing up to 0.3 g/sec. On the other hand, with decreasing diameter to 10 mm the frequency of fundamental oscillations decreases to 3 kHz. In nitrogen and argon the fundamental oscillations frequency in channels with a plasma equals, respectively, 2.5 and 8.0 kHz. In smooth 8 mm slotless channels the oscillation frequency of an argon arc increases to 15 kHz. Under our experimental conditions the gas twist and the channel length exerted no noticeable effect on the nature of oscillations of the arc column.

Analysis of the photorecordings shows that the plasma column oscillates as a whole without substantial size changes.

**Oscillations of Radiation Intensity and Temperature.** Intensity fluctuations of the radiant flux are caused by both perturbations in the arc column parameters and by its transport during the recording of radiation from the arc oscillating in the channel. The column oscillation frequency reaches $2 \cdot 10^4$ Hz. To isolate in this case the oscillation emerging from the arc radiation flux, measurements are required of the radiant flux with temporal resolution better than $10^{-5}$ sec. This possibility was guaranteed by fast photography of interferograms with a frequency up to $2.5 \cdot 10^5$ $\sec^{-1}$. Also investigated was the possibility of using simple model representations of radiation intensity distribution functions over radius in the channel and in the arc.

If the radiation intensity distribution function in the arc column I(x) and the column oscillation distribution in the channel $\varphi$(y) are known, one can calculate the intensity distribution function in the channel J(y).

In the "Gauss–Gauss" model it is assumed that J(y) and $\varphi$(y) have normal distributions with halfwidth A and dispersion $\sigma$. I(x) is then also a Gaussian function with maximum value $I_0$ and halfwidth $a$:

$$I(x) = I_0 \exp\left(-\frac{x^2}{2a^2}\right), \tag{1}$$

$$I_0 = J_0\Theta, \tag{2}$$

$$a = (A^2 - \sigma^2)^{1/2}, \tag{3}$$

where

$$\Theta = \frac{A}{a} = (1 - n^2)^{-1/2}, \tag{4}$$

$$n = \frac{\sigma}{a}. \tag{5}$$

To verify the validity of the "Gauss–Gauss" model, experimental studies were carried out of "instantaneous" radiation intensity contours in the arc I(x) and of the mean values of the radiation intensity distribution in the channel J(y). Figure 2 shows the experimental profiles of $I(x)/I_0$ and $J(y)/J_0$, approximating the Gaussian profiles (1) and

$$J(y) = J_0 \exp\left(-\frac{y^2}{2A^2}\right), \tag{6}$$

plotted by solid lines. Besides, the dashed lines show profiles of the form:

$$I(x) = I_0 \exp\left(-\frac{x^2}{2a^2} - \beta\frac{x^4}{a^4}\right), \tag{7}$$

$$J(y) = J_0 \exp\left(\frac{y^2}{2A^2} - \beta\frac{y^4}{A^4}\right), \tag{8}$$

where $\beta$ is the parameter of deviation from a normal distribution. The function I(x) characterizes the integral of the arc radiation over the spectrum, basically determined by atomic and continuum lines.

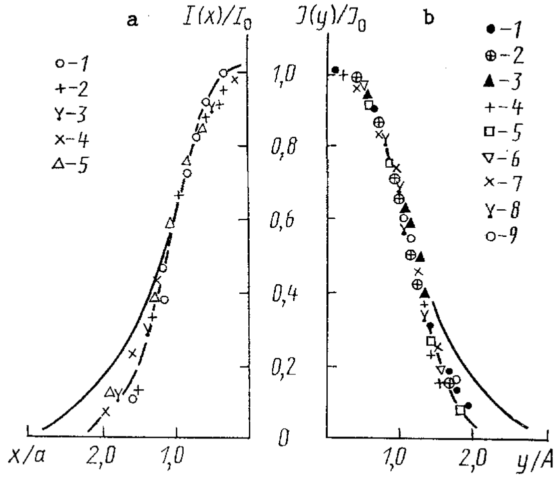


Fig. 2. Radiation profiles of an oscillating electric arc: a) instantaneous profile, integral radiation, temporal resolution $10^{-5}$ sec, solid line – Gaussian distribution, dashed line – the approximation $I(x) = I_0\exp(-x^2/2a^2 - \beta x^4/a^4)$, d = 0.8 cm; 1) I = 150 A, G = 0.3 g/sec; 2) 120 and 1.5; 3) 100 and 1; 4) 80 and 1; 5) 60 and 1; b) average profile, temporal resolution 8 sec, solid line – Gaussian distribution, dashed line – the approximation $J(y) = J_0\exp(-y^2/2A^2 - \beta y^4/A^4)$; 1) d = 1 cm, I = 120 A, G = 1.5 g/sec, ArII 480.6 nm; 2) d = 1 cm, I = 160 A, G = 1.0 g/sec, ArI 430.0 nm; 3) d = 0.8 cm, I = 60 A, G = 1.0 g/sec, ArI 852.2 nm; 4) d = 0.8 cm, I = 150 A, G = 2.0 g/sec, NI 742.3 nm; 5) d = 0.8 cm, I = 100 A, G = 1.5 g/sec, NI 742.3 nm; 6) d = 0.8 cm, I = 160 A, G = 0.2 g/sec, HeI 492.3 nm; 7) d = 0.8 cm, I = 160 A, G = 0.2 g/sec, HeI 501.6 nm; 8) d = 0.8 cm, I = 150 A, G = 2.0 g/sec, OI 882.0 nm; 9) d = 0.8 cm, I = 150 A, G = 2.0 g/sec, NII 463.0 nm.

As seen from Fig. 2, Gaussian functions describes quite well the central part of the profile, and differ somewhat from the experimental points in the contour tails. Under the assumptions made, the dispersion distribution of radiative flux oscillations over the radius of the channel is

$$\Delta J^2(y) = J^2(y)\left[\frac{1+\Delta\bar{I}_0^2/\bar{I}_0^2}{\sqrt{1-n^2}}\exp\left(\frac{y^2}{A^2}\frac{n}{n+1}\right)-1\right]. \tag{9}$$

Calculations by Eq. (9) show that a trough is observed on the chamber axis, while the oscillations decrease at the periphery. The maximum of the curve is shifted by some distance from the axis for $0 < \sigma/a < 0.84$. In the general case, in the presence of oscillations int he column we have

$$y_m^2 = A^2\frac{n+1}{n}\ln F, \tag{10}$$

where

$$F = \frac{(1+n)\sqrt{1-n^2}}{1+\Delta\bar{I}_0^2/\bar{I}_0^2}. \tag{11}$$

The expressions obtained can be used to determine the relative radiation intensity oscillations inside the oscillating arc column $\Delta I_0^2/I_0^2$ without carrying out complicated measurements of intensity fluctuations with high temporal resolution. For this purpose one can measure the radiation intensity and the dispersion of its oscillation at the center of the channel and at some distance from the center. A simple dependence is obtained at the distance $y_m$

$$\Delta\bar{J}^2(y_m) = n\bar{J}^2(y_m). \tag{12}$$

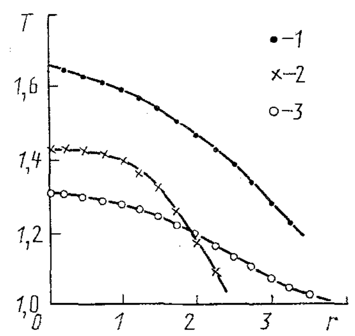


Fig. 3

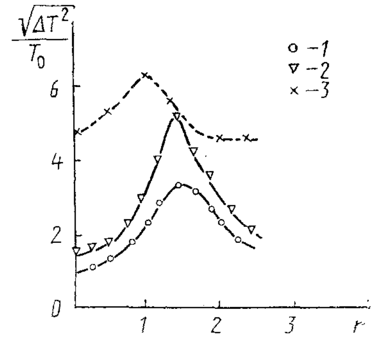


Fig. 4

Fig. 3. Temperature profiles of an arc, blown by different gases: 1) helium (HeI, 492.3 nm), 2) air (NI, 742.3 nm), 3) argon (ArII, 480.6 nm) T, K $\cdot 10^4$; r, mm.

Fig. 4. Mean-square relative temperature fluctuations in turbulent arcs: 1) argon, 2) air, 3) argon from [7]. $\sqrt{\Delta T^2}/T_0$, %.

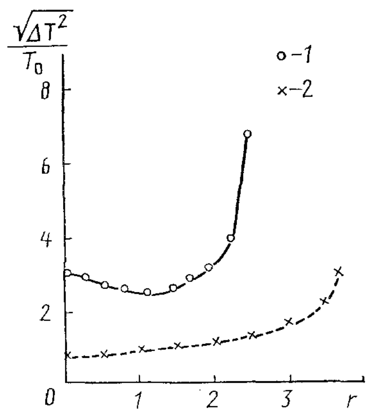


Fig. 5. Mean-square relative temperature fluctuations in laminar arcs: 1) helium, 2) argon.

The volume radiative capability $\varepsilon(r)$ drops quickly with increasing r. Therefore, the major part of the measured radiant flux is formed in the central layer $\Delta y \approx A$. One can correspondingly simplify the measurement process of relative oscillations of the radiative capability, putting

$$\left.\frac{\sqrt{\overline{\Delta\varepsilon^2(r)}}}{\bar{\varepsilon}(r)}\right|_{r=x} = \frac{\sqrt{\overline{\Delta I^2(x)}}}{I(x)}. \tag{13}$$

The temperature oscillations can be determined from the oscillation in the radiative capability with sufficient practical accuracy, using the dependence

$$\frac{\sqrt{\overline{\Delta T^2}}}{\bar{T}} = \frac{kT}{E_n}\,\frac{\sqrt{\overline{\Delta\varepsilon^2}}}{\bar{\varepsilon}}. \tag{14}$$

Figure 3 shows the experimental profiles of the mean temperature $\bar{T}(r)$, while Figs. 4 and 5 provide the mean-square deviation profiles of its fluctuations $(\Delta\bar{T}^2(r))^{1/2}/\bar{T}_0$ for arcs heated in an atmosphere of argon, helium and air in the turbulent and laminar flow regimes, respectively. The shape of the fluctuation distribution function shows that in air and argon, for these gas discharges the arc oscillates, while it is fixed in helium. At the same time one observes in helium temperature oscillations in the arc column. The oscillation intensity drops initially from the arc axis toward the periphery, but starts increasing again at the edge of the column. In the air and argon atmosphere the temperature oscillations are primarily created due to displacements of the arc column.

**2. Correlation of Characteristic Arc Discharges. Criteria of Energy Exchange.** Establishing the presence of turbulent energy transport in an electric arc is possible by generalizing its energy characteristics. The essence of the method consists of the fact that each form of energy transport is characterized by some dimensionless number (criterion). The experimental data in arc energy characteristics correlate with a sequence of such numbers used s dimensionless arguments, characterizing different types of energy transport. A minimum spread in experimental points is obtained in that generalized characteristic in which the number characterizing the dominant energy transport process is used for the correlation. Obviously, in the presence of thermal turbulence in the blown arc turbulent energy transport must play a substantial role.

Dimensionless numbers, determining the different types of energy transport, were already obtained in the sixties [10-13]. At the same time, however, the turbulence problem was not especially treated, and the number characterizing turbulence was provided substantially later [3, 4]. For the basic types of energy transport in a longitudinally blown arc the dimensionless numbers are:

$$\Pi_1 = \frac{\lambda_0 \sigma_0 T_0 R^2}{I^2} \tag{15}$$

– the conductive heat release energy of Joule dissipation,

$$\Pi_2 = \frac{\sigma_0 h_0 G R}{I^2} \tag{16}$$

– the convective heat release energy of Joule dissipation ("blown-through" arc),

$$\Pi_3 = \frac{\sigma_0 Q \;\; R^4}{I^2} \tag{17}$$

– the heat release energy of Joule dissipation by bulk radiation, and

$$\Pi_4 = \frac{\rho_0 \sigma_0 h_0^{1,5} R^3}{I^2} \tag{18}$$

– the turbulent heat release energy of Joule dissipation (the criterion of thermal turbulence).

The $\Pi_1 - \Pi_3$ criterion can be obtained by reducing the energy equations for an electric arc [11-13] to dimensionless form or by a dimensionality analysis method. They express the ratio of the power removed per unit volume by the corresponding method to the power of Joule dissipation. In analogy with these numbers the criterion of thermal turbulence $\Pi_4$ must also express the ratio of the power removed from the arc by means of turbulent fluxes to the power of Joule dissipation. The energy equation for this case is

$$\operatorname{div} \rho v h = j^2/\sigma. \tag{19}$$

Hence is obtained the dimensionless number $\sigma_0 \rho_0 v_0 h_0 R^3/I^2$. The scale values of the physical properties $\sigma_0$, $\rho_0$, $h_0$ can be determined from their temperature dependences [14]. The radius of the discharge channel and the current are assumed known. It is necessary to clarify how the mean velocity is formed during turbulent energy transport under conditions of electric arc discharge.

Turbulent energy transport is realized in a temperature field gradient. The mechanism of gas acceleration due to its thermal energy in nozzle – exit cone nozzles is well known. In this case the flux rate at the nozzle outlet is $v \sim \sqrt{\Delta h}$. It is also well known [15] that besides geometric nozzles thermal gas acceleration is possible in thermal and discharge nozzles. The formation of such thermal and discharge nozzles in regions of chaotic plasma heating is quite possible. In this case the scale of turbulent globules in the arc is comparable with the channel radius. For the velocity scale one can then take $v_0 = \sqrt{h_0}$. The criterion $\Pi_4$ is correspondingly obtained from (19).

**CVC Correlations.** The CVC experimental data of arc discharges were generalized in the form $UR\sigma_0/I = K_t \Pi^{\alpha_i}$. For the same data we compared the values of the mean-square deviations during correlation in one of the generalized arguments $\Pi_i$. Table 1 provides values of the relative mean-square deviations for correlated CVC of a plasmotron with cylindrical hollow electrodes and longitudinally vortical arcs blown by different gases. It is seen from the table that in all gases, except helium, convective heat exchange is predominant, in which case the dissipation energy is removed by the flux "blown" through the gas

TABLE 1. Dependence of Relative Mean-Square Deviation of the Generalized Stress $UR\sigma_0/I$ during Correlation of Generalized CVC in Arcs with Weak Longitudinal-Vortical Inblow by Various Gases

| Generalized argument | Mean-square deviation | | | | |
|---|---|---|---|---|---|
| | air | nitrogen | hydrogen | argon | helium |
| $\Pi_1$ | 0,619 | 0,274 | 0,472 | 0,298 | 0,475 |
| $\Pi_2$ | 0,334 | 0,194 | 0,103 | 0,268 | 0,426 |
| $\Pi_3$ | 0,679 | 0,377 | 0,574 | 0,343 | 0,402 |
| $\Pi_4$ | 0,467 | 0,308 | 0,302 | 0,289 | 0,382 |

TABLE 2. Relative Mean-Square Deviations of the Generalized Stress during Correlation of Generalized CVC in Weakly Stabilized Transversally Blown Arcs

| Generalized argument | Mean-square deviation | | | |
|---|---|---|---|---|
| | air | hydrogen | argon | helium |
| $\Pi_1 = \frac{\lambda_0 T_0 \sigma_0 \delta^2}{I^2}$ | 0,173 | 0,426 | 0,352 | 0,252 |
| $\Pi_2 = \frac{\rho_0 h_0^2 \sigma_0^2 \delta^5 B}{I^3}$ | 0,068 | 0,295 | 0,453 | 0,177 |
| $\Pi_4 = \frac{\rho_0 \sigma_0 h_0^{1,5} \delta^3}{I^2}$ | 0,116 | 0,270 | 0,445 | 0,208 |

discharge. Heat release by means of turbulent energy transport is predominant in helium. This result is in good agreement with experimental data on temperature instabilities. It is precisely in a helium arc that the increase in temperature fluctuations at the center of a longitudinally blown arc is observed.

On the other hand, comparison of the mean-square deviations in the separate criteria for each of the operating media shows that even when turbulent energy exchange is not predominant it plays a substantial role. In most cases the spread in data for $\Pi_4$ correlations is smaller than for $\Pi_1$ (conductive heat exchange). Possibly, here one deals with precisely peripheral turbulization of the arc column in the region of large temperature gradients.

Table 2 provides data of the similar CVC correlation of transversally blown arcs, rotating under the action of a magnetic field in the blown-through gap between concentric electrodes. Arcs of this type differ substantially in instability, as well as high-level fluctuations of electric parameters.

In this case is also seen the substantial effect of turbulent energy transport. But, unlike the longitudinally blown arc, the predominant $\Pi_4$ criterion occurred in the hydrogen arc. Evidently, there is a substantial difference between longitudinally and transversally blown arcs in the nature of formation of temperature instabilities. In transversally blown arcs the probable instability sources are processes of hydrodynamic, not thermal, character.

The good CVC correlation in the criterion of "thermal turbulence" $\Pi_4$ justifies the assumption that the temperature instabilities generated by the formation of chaotic micronozzles lead to generation of turbulent mass fluxes, by whose means the corresponding energy transport is implemented.

**Analysis of the Thermal Turbulence Number.** In the data considered of CVC correlation results some difference persists in the operating media, in which turbulent energy transport was predominant. In this context it is interesting to consider the absolute values of the turbulence number for the different gases. In Fig. 6 we show the temperature dependence of the turbulent number $\Pi_4$ for different gases. It seems that its largest value belongs to hydrogen. This result is in good agreement with data of the generalized CVC of transversally blown arcs. For helium, strangely enough, this number seems to be the smallest. Evidently, further study is needed to explain the paradox mentioned. Here, however, one can suggest one explanation, which is found within the model considered of micronozzle formation and is quite credible.

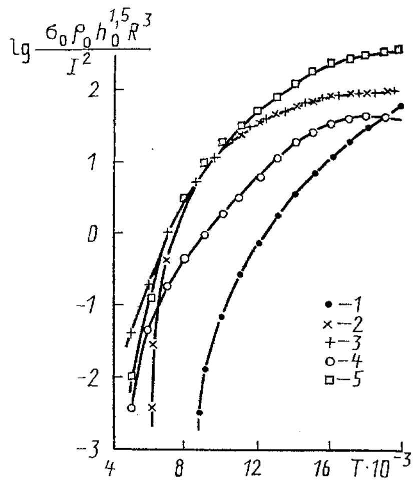


Fig. 6. Temperature dependence of the criterion $\rho_0\sigma_0 h_0^{1.5}R^3/I^2$, channel diameter 4 mm, current 500 A: 1) helium, 2) nitrogen, 3) air, 4) argon, 5) hydrogen. T, K.

The condition of action reversal for a thermal nozzle [15] can be written in the form

$$(1 - M^2)\frac{dv}{v} = \frac{dQ}{\rho h}. \tag{20}$$

If $\tau$ and $l$ are the temporal and spatial turbulence scales, the thermal source is $Q = \tau j^2/\sigma$ and $l \sim \tau\sqrt{h}$. For $R \approx l$ one can then obtain from (20) the number $\Pi_5 = I/\Pi_4 = I^2/\sigma_0\rho_0 h_0^{1.5}R^3$. It hence follows that the higher the thermal gas acceleration, the smaller $\Pi_4$, i.e., it must be largest for helium. During the formation of thermal micronozzles the average velocity of turbulent fluxes increases with decreasing $\Pi_4$, with heat transport consequently increasing. The thermal flux reaches a maximum at some value of the number $\Pi_4$, and then starts reducing. Instabilities of transversally blown arcs are due to nonthermal effects. Therefore, the more intense the turbulent heat transport, the larger the number $\Pi_4$.

The following conclusions can be drawn from the study carried out.

1. A longitudinally blown electric arc in a laminar flow generates turbulent perturbations at the periphery of the arc column. This turbulence decays in the direction of the arc axis due to the high viscosity of the arc plasma.

2. In unstable arcs the temperature oscillations create local regions of plasma heating – energy sources for acceleration of turbulent jets. These jets are a means of energy transport inside the arc. In a number of cases the energy transport resulting from this mechanism can be predominant among the remaining types of heat exchange.

3. The hydrodynamic mechanism is not the only means of turbulization of electric arcs. Along with it there exists a destabilization factor due to heating instabilities. So far it has been noticed distinctly only in a helium arc, and special experiments are required to explain its effect in other media.

## NOTATION

A and $a$, halfwidths of the contours J(y) and I(x), respectively; B, magnetic induction; $E_n$, energy level; G, gas discharge; h, enthalpy; measured by the depth; I, current intensity; I(x), radiation intensity in the arc column; J(y), radiation intensity in the channel discharge; j, current density; K, a coefficient; k, Boltzmann constant; $l$, channel length, the spatial scale of turbulence; M, Mach number; Q, thermal energy source; $Q_{r0}$, integral bulk radiation; R, r, channel radius; T, temperature; U, arc intensity; v, velocity; $\beta$, deviation parameter of the radiation intensity from the normal law; $\delta$, gap between concentric electrodes; $\varepsilon$, radiative capability; $\varphi$(y), probability of transverse displacements of the arc column; $\lambda$, thermal conductivity; $\Pi$, a dimensionless criterion; $\rho$, density; and $\sigma$, electric conductivity, the relative mean-square deviation of the function $\varphi$(y).

## LITERATURE CITED

1. O. I. Yas'ko, Electric Arcs in a Plasmotron [in Russian], Minsk (1977).
2. M. F. Zhukov, A. S. Koroteev, and B. A. Uryukov, Applied Dynamics of a Thermal Plasma [in Russian], Novosibirsk (1975).
3. V. A. Vashkevich, S. K. Kravchenko, and O. I. Yas'ko, in: Proc. IX All-Union Conf. Generation of Low-Temperature Plasma [in Russian], Frunze (1983), pp. 56-57.
4. S. K. Kravchenko, T. V. Laktyushina, and O. I. Yas'ko, in: Proc. IX All-Union Conf. Generation of Low-Temperature Plasma [in Russian], Frunze (1983), pp. 58-59.
5. A. V. Nedopasov and V. D. Khait, Oscillations and Instabilities in a Low-Temperature Plasma [in Russian], Moscow (1979).
6. V. I. Artemov, Yu. S. Levitan, and O. A. Sinkevich, Pis'ma Zh. Tekh. Fiz., **10**, No. 7, 413-416 (1984).
7. Y. K. Chien and D. M. Benenson, IEEE Trans. Plasma Sci., **PS-8**, No. 4, 411-417 (1980).
8. E. A. Kostjukevich and G. P. Lizunkov, "A cuvette interferometer: design and field of application," Interferometry-89, Warsaw (1989).
9. G. P. Lizunkov, V. P. Kabashnikov, A. A. Kurskov, and V. D. Shimanovich, "Methods of spectroscopic diagnostics of a nonstationary arc plasma on the basis of simulating its oscillations," Minsk (1986), Preprint Inst. Fiz. Akad. Nauk Belarus. SSR, No. 446.
10. S. S. Kutateladze and O. I. Yas'ko, Inzh.-Fiz. Zh., **7**, No. 4, 25-27 (1964).
11. O. I. Yas'ko, Inzh.-Fiz. Zh., **7**, No. 12, 112-116 (1964).
12. O. I. Yas'ko, Inzh.-Fiz. Zh., **15**, No. 4, 165-169 (1968).
13. O. I. Yas'ko, Brit. J. Appl. Phys. (J. Phys. D), Ser. 2, **2**, 733-751 (1969).
14. O. I. Yas'ko, Pure Appl. Chem., **62**, No. 9, 1817-1824 (1990).


# EVOLUTION OF PERTURBATIONS IN A HIGH-PRESSURE NON-SELF-SUSTAINING DISCHARGE

**A. F. Pal' and A. N. Starostin**

UDC 537.521.7

*An experimental and numerical investigation is conducted of the evolution of perturbations, which are excited in a non-self-sustaining discharge, which is controlled by an electron beam at pressures close to atmospheric in various gases and gas mixtures. The perturbations were generated by the discharge itself or with the aid of a specifically introduced external source. As a result, spatially inhomogeneous structures arise, which are oriented along or transverse to the electric field and which degrade the optical properties of the active medium created by the discharge.*

A high-pressure, non-self-sustaining discharge which is controlled by an electron beam makes it possible to obtain an active medium of practically unlimited cross section. Such a medium is constantly subjected to the action of external perturbations, which locally change some of its parameters. Local deviations from average values of macroscopic characteristics are also constantly generated within the medium. Stationary and transient structures are formed during development of the excited perturbations. Therefore a homogeneous plasma exists only for a rather short time in an experiment, thereby limiting its possible applications.

---

I. V. Kurchatov Institute of Atomic Energy, Moscow. Translated from Inzhenerno-Fizicheskii Zhurnal, Vol. 62, No. 5, pp. 701-706, May, 1992. Original article submitted November 12, 1991.